APEX INITIAL COMMISSIONING RESULTS*

D. Filippetto†, B. Bailey, K. Baptiste, J. Corlett, C. Cork, S. De Santis, S. Dimaggio, L. Doolittle, J. Doyle, G. Huang, H. Huang, T. Kramasz, S. Kwiatkowski, R. Lellinger, V. Moroz, W.E. Norum, C. Pappas, C.F. Papadopoulos, G. Portmann, C. Pogue, F. Sannibale, J. Staples, M. Vinco, R. Wells, M. Zolotorev, F. Zucca, LBNL, Berkeley, CA94720, U.S.A.

Abstract

APEX, the Advanced Photo-injector Experiment at the Lawrence Berkeley National Laboratory, is devoted to the development of a MHz-class repetition rate high-brightness electron injector for X-ray FEL applications. The injector is based on a new concept photocathode gun utilizing a room-temperature 186 MHz RF cavity operating in CW mode in conjunction with high quantum efficiency semiconductor photocathodes capable of delivering the required charge at repetition rates consistent with commercially available laser technology. APEX is organized in three main phases. Phase 0 demonstrates several important milestones for the project: gun cavity conditioning to full RF power in CW mode to demonstrate the required field at the cathode; the gun vacuum performance impacting the lifetime of photo-cathodes; and tests of several different photocathodes at full repetition rate at the nominal gun energy of 750 keV. Phase I, continues cathode studies with a new suite of beam diagnostics added to characterize the electron beam at the gun energy and at full repetition rate. In Phase II, a pulsed linac will be added for accelerating the beam to several tens of MeV to reduce space charge effects and measure the high-brightness performance of the gun when integrated in an injector scheme. Phase 0 is presently under commissioning, and the first experimental results from this phase are presented.

INTRODUCTION

The construction of several linac based MHz repetiton rate facilities serving multiple independent FELs has recently been proposed [1, 2, 3, 4], supported by a strong demand from FEL users [5], to be able to extend FEL performance to MHz and beyond, allowing for experiments where large statistical samples are required, and dramatically decreasing the time required to perform experiments.

The APEX project is aiming to the construction and test of an high repetition rate (MHz) high brightness photogun capable of producing bunches with brightness high enough to drive an X-ray FEL, but with an average current 10^4 times higher than the present rf guns. The successful normal-conducting (NC) high-frequency (greater than 1 GHz) high-brightness technology used in present low repetition rates X-ray FEL RF guns [6] can indeed not be scaled to repetition rates beyond $\sim$ 10 kHz because the heat load due to Omhic losses in the gun cavity becomes too large for being dissipated by the cooling system [7]. Many alternative electron gun schemes and technologies are being pursued around the world in order to achieve the required brightness at high repetition rates [8] but at the present time none have demonstrated the necessary set of requirements [9].

The Advanced Photo-injector EXperiment (APEX) [10] is designed to fill that gap by developing a gun and an injector capable of the required performance. The gun, based on a novel concept [11, 12], has been fabricated and recently completed the first phase of its commissioning. All the performance milestones included in this part of the project were successfully achieved and this paper reports the results of the related tests.

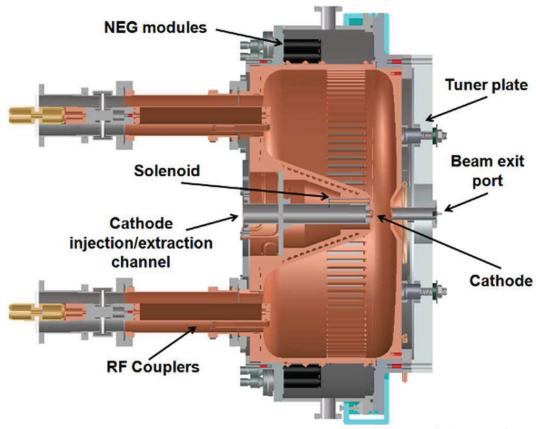

Figure 1: APEX VHF Gun cross section with main components.

APEX, THE ADVANCED PHOTO-INJECTOR EXPERIMENT

APEX is an electron injector built around a RF photogun based on reliable and mature mechanical and RF technologies. The core of the gun is a NC copper RF cavity operating in continuous wave (CW) mode in the VHF band at 186 MHz. The frequency value is chosen to be close to either the 7^{th} sub-harmonic of 1.3 GHz or the 8^{th} subharmonic of 1.5 GHz, making the gun operation compatible with both of the main super-conducting electron linac technologies presently available [13, 14].

Figure 1 shows a CAD cross section of the cavity with its main components, and Table 1 contains the VHF gun main design parameters selected to satisfy the requirements set in reference [9]. The resonant copper structure is sur-

* Work supported by the Director of the Office of Science of the US Department of Energy under Contract No. DEAC02-05CH11231

† Dfilippetto@lbl.gov

ISBN 978-3-95450-123-6

Table 1: VHF Gun Main Design Parameters

Parameter	Value
Frequency (MHz)	186
Operation mode	CW
Nominal beam energy (MeV)	0.75
Field @ cathode during emission (MV/m)	19.47
Ideal conductor quality factor, Q_0	30900
Shunt impedance (MΩ)	6.5
Nominal RF power for Q_0 (kW)	87.5
Stored energy (J)	2.3
Maximum surface field (MV/m)	24.1
Maximum wall power density (W/cm^2)	25.0
Accelerating gap (cm)	4
Cavity inner diameter (cm)	69.4
Cavity length (cm)	35.0
Operating pressure (Torr)	$\sim 10^{-11}$

rounded by a stainless steel shell that ensures the necessary mechanical rigidity and the proper vacuum envelope. No sliding tuner is present and the required frequency tuning is achieved by a mechanical system that slightly pushes or pulls the cavity wall at the beam exit port side. The RF power is supplied through two magnetic loop couplers diametrically opposed on the cathode back wall of the cavity. A vacuum load lock system, based on the INFN design [15] (used at the FLASH and PITZ facilities in Germany) allows the replacement and/or the *in situ* conditioning of photocathodes without breaking the vacuum in the gun.

More details on the gun can be found elsewhere [10, 11, 12], here we want just to remark that the two major goals targeted by the gun design are the CW operation, and the low-vacuum performance ($10^{-11} - 10^{-9}$ Torr) necessary to operate with acceptable lifetime high quantum efficiency (QE) semiconductor photocathodes sensitive to ion back-bombardment and contamination. Such cathodes are required to generate the desired charge per bunch at high repetition rate with the power available by present laser technology.

The relatively low RF frequency choice for the VHF gun has addressed both of these needs. The larger resonating structure associated with the VHF frequency decreases the power density on the cavity walls to a level small enough to permit CW operation with conventional cooling techniques while maintaining the high electric fields required for the high brightness performance. Additionally, the long wavelength allows opening large slots visible on the cavity walls in Figure 1 with negligible field distortion, thereby creating an extremely high vacuum conductance connecting to the pumping system located in the plenum around the cavity equator. Twenty 400 l/s commercial NEG pumps (SAES CapaciTorr®-D 400-2) ensures a formidable pumping of cathode contaminating molecules (H_2O, O_2, ...), while a 400 l/s ion pump connected to the bottom of the plenum removes noble gasses and residual hydrocarbons.

The choice of the accelerating gradient for the VHF gun represents a tradeoff between contrasting requirements. From one side, beam dynamics considerations push towards higher gradients, while minimizing dark current (due to field emission) demands relatively low gradient. Mitigating dark current from the gun in a high repetition rate facility is of particular importance for avoiding undesired radiation losses along the main linac, and the risk of "quenching" downstream superconductive accelerating sections. Extensive beam dynamics simulations [16] showed that the gradient value in Table 1 for the VHF gun allows delivering the required brightness performance, and comparison with dark current vs gradient data for existing guns [17] jointly with initial dark current tracking studies for an FEL application [18] indicate also that the selected gradient should keep dark current at tolerable levels.

APEX is staged in three phases. Phase 0, illustrated in Figure 2, consists of the VHF gun and a diagnostic beamline for cathode characterization. The primary scope of this phase is to commission the VHF gun and validate the technological choices used for it. A number of fundamental milestones need to be demonstrated in this critical phase, including full CW RF conditioning of the gun cavity, achievement of the design gradient at the cathode and associated beam energy at the gun exit, demonstration of the challenging vacuum performance, and characterization of dark current from the gun. Phase 0 also includes a photocathode R&D program in which different materials will be tested at MHz repetition rate at the gun energy to define the best choice for a high repetition rate X-ray FEL.

In Phase I an electron beam diagnostic suite [19] is added to the Phase 0 layout, to allow a full 6D characterization of the beam phase space at MHz repetition rate and at the nominal gun exit energy. The diagnostic suite includes among other components, a two-slit emittance measurement system (to measure the emittance in the space charge dominated regime), a transverse deflecting cavity (both based on a modified Cornell design [20, 21]) and a spectrometer for slice emittance and energy spread measurements and full longitudinal phase space characterization.

In Phase II a 1.3 GHz room temperature pulsed linac (using 3 ANL-AWA accelerating sections [22]) and a room temperature 1.3 GHz buncher cavity (a scaled version of the Advanced Light Source harmonic cavity [23]) are added to the Phase I layout. The electron beam diagnostic suite of Phase I (after some modification) is moved downstream of the linac. The new linac system will accelerate the beam up to ∼30 MeV making space charge forces sufficiently small to perform reliable measurements of beam brightness while also compressing the bunch to the required length.

Phase 0 beamline installation is completed, Phase I components are under fabrication, and initial design and specification of components and layout for Phase II are underway.

ISBN 978-3-95450-123-6

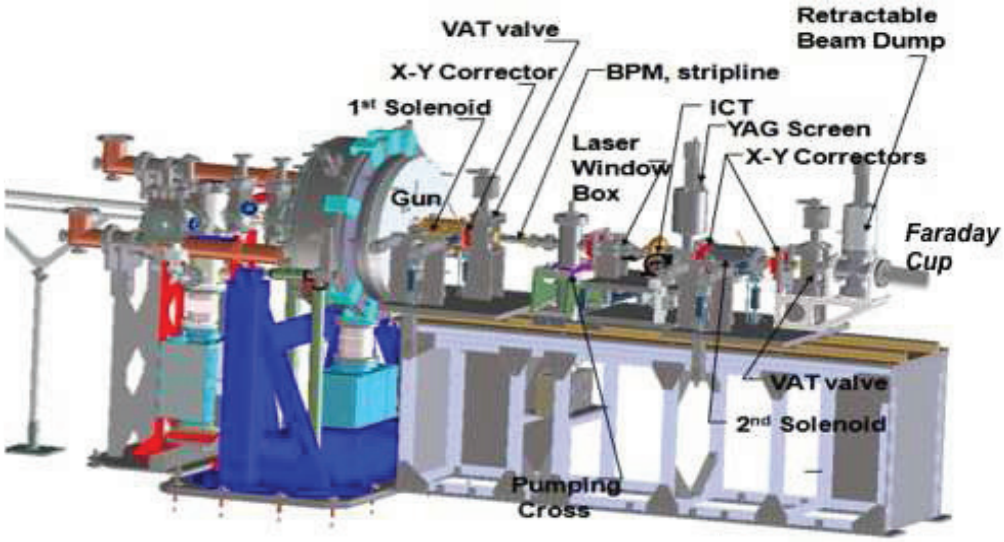

Figure 2: APEX Phase 0 Layout. The about 2.5 m long beamline allows to characterize and test cathodes at MHz repetition rates at the nominal gun energy of 750 keV.

The Laser System

The laser system is based on a diode-pumped Yb doped fiber oscillator, with a repetition rate of 37.2 MHz providing hundreds of pJ pulses with sub-picosecond duration at 1060 nm [24]. The infrared pulse is then stretched and amplified, and the repetition rate is lowered down to 1 MHz. About 0.65 μJ are obtained in a 600 fs full width half maximum (FWHM) after the final amplification re-compression stage. The laser is fiber guided throughout the amplification stages until the final compressor (a grating pair), where the peak power becomes too high and transport in air is necessary. The system has been provided by Lawrence Livermore National Laboratory (LLNL).

After the compression a 3 mm non-critically-phase-matched LBO crystal (heated up to 180 °C) is used to generate the second harmonics @ 530 nm with 35% efficiency (240 nJ). Type I phase matching in a 1.5 mm BBO is then used to up-conversion of green to UV (265 nm) with 25% efficiency.

One of the APEX goals is the test of different cathode materials in an CW rf environment. Among the possible candidates, Cesium Telluride (Cs_2Te) and Multi-Alkali CsK_2Sb) [25] cathodes are very attractive because of their high quantum efficiency (>1%) and low intrinsic emittance. Both cathodes will be tested at APEX and, because of their different photoemission energies, both UV and green light are generated and transported to the gun at the same time.

Depending on the electron beam charge requested, the laser pulse length optimum may vary from 1 ps to 50 ps. The pulse stacking technique [26] is used for the pulse shaping and tests in the UV are already started, using a series of 6 αcut BBO crystal flat-top pulses [27]. The same technique will be used in the green. A high voltagePockels cell (KDP crystal) is used in conjunction with a polarizer beam splitter as fast shutter to control the laser repetition rate.

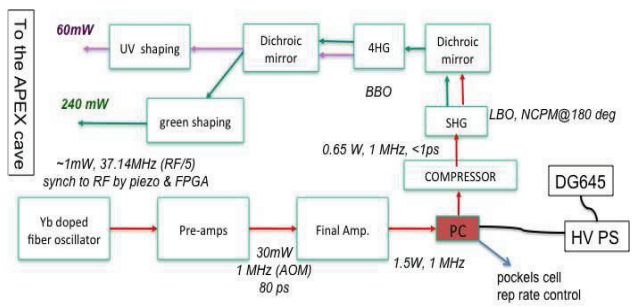

Figure 3: The APEX laser system layout. Two separate lines transport the UV and the green laser pulses down to the gun area.

The laser-to-rf synchronization is assured by a feedback loop with a piezo actuator in the laser oscillator to control the cavity length (20KHz bandwidth), and a Phase locked loop implemented in the low level RF board (FPGA based, [28]), that creates an error signal proportional to the difference between the RF gun cavity frequency and the laser oscillator frequency. The measured closed-loop jitter is shown in Figure 4. The root mean square value (RMS) 2 ps, corresponding to about 0.15 rf degrees at 186 MHz, and is therefore more than what we need for the first phase of the project. Improvements will be needed for phase I and II, when higher frequency cavities will be installed.

The location of the laser system is on the top of the shielding area of APEX. The distance from the laser system to the photo-injector cathode is about 12m and the designed beam transport uses Relay imaging to transport the pulses up o the final table, where a final point-to-point imaging to the cathode is performed. A total of 4 long focal length lenses is used up to the cathode plane.

ISBN 978-3-95450-123-6

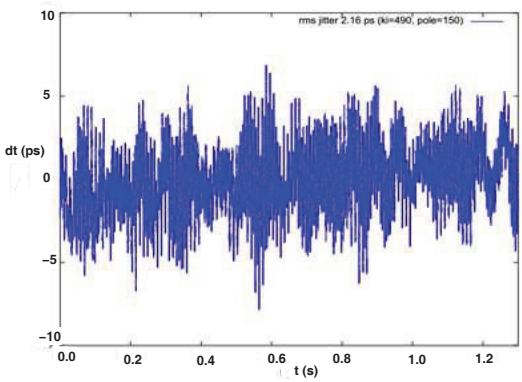

Figure 4: Measurement of laser-to-RF jitter in closed loop. The measured RMS value is 2ps.

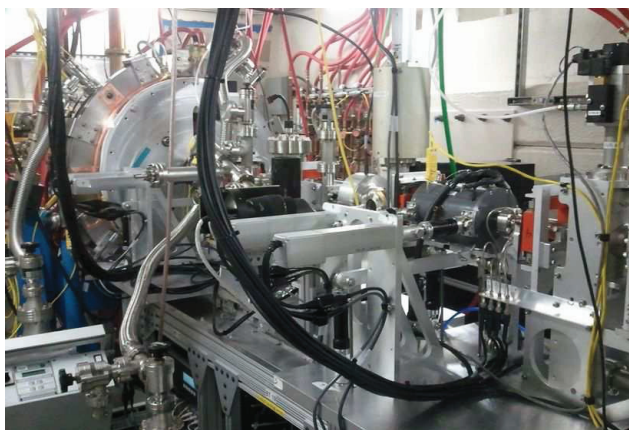

Figure 5: APEX Phase 0 installed in the Beam Test Facility at the Advanced Light Source.

APEX PHASE 0 COMMISSIONING RESULTS

Currently, all Phase 0 hardware (with the exception of the vacuum loadlock system) has been installed. Figure 5 shows the beamline in the test area. The beam diagnostics included in the present layout allows for the measurement of beam current, energy and transverse profile, and of cathode QE maps, intrinsic emittance and lifetime [19].

The photocathode drive laser has been installed and fully commissioned. The 120 kW 186 MHz CW RF source for the gun (fabricated by ETM Electromatic Inc.) is fully operational and reliably delivering the required power to the gun through two 60 kW tethrodes (Thales TH571B). The power level stability of the system is $\sim 10^{-3}$ rms when controlled by a high level software feedback.

The EPICS based control system is in an advanced stage of implementation and permits the full control of the beamline components and acquisition of experimental data. High level macros developed in MatLab® on linux platforms allow for a flexible system operation and experiment control.

The FPGA-based low-level RF system (LLRF) is developed at LBNL and allows control of the RF system, synchronization with the laser, and tuning of the frequency of the RF source to follow the cavity frequency [28].

VHF Gun Cavity Low and High Power RF Tests

In the summer of 2010 the gun fabrication was completed and the low power RF tests were performed. The measured resonance frequency was in agreement with the expected value, and the measured cavity quality factor Q, was $\sim 86\%$ of the ideal conductor case demonstrating the excellent quality of the cavity fabrication and the accuracy of the design model. With the measured Q value, ~ 100 kW of RF power are required to accelerate the beam to the nominal energy of 750 keV, well within the capability of the VHF RF source.

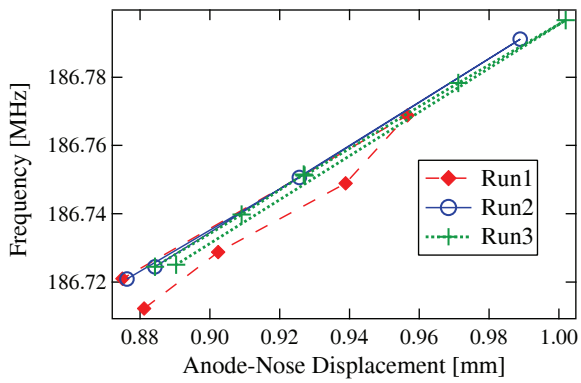

Figure 6: Fundamental mode frequency shift vs. "anode" wall cavity displacement induced by the tuner system.

The frequency shift induced by pulling (or pushing) the cavity wall on the beam exit side, important for calibrating the action of the mechanical tuner, was also measured. Figure 6 shows the very first three runs of measurements. After some settling of the mechanical parts observable in the first run, the second and third runs showed a linear and reproducible frequency dependence on the wall displacement. Linear fits of Run 2 and Run 3 points give a slope of ~ 630 kHz/mm, in good agreement with simulation predictions. The actual displacement (and hence the natural cavity frequency) will be remotely set by heavy duty piezomotors controlled by the LLRF system.

After installation in the beam test facility, and commissioning of the high power CW source, at the end of 2011 the gun cavity was successfully conditioned at the nominal power of 100 kW in CW mode after only ~ 150 integrated hours of conditioning. This important result confirmed the capability of the gun of operating at the required fields without RF breakdown. Continuous runs of more than 30 hours duration with no faults showed a solid reliability of the RF system. As predicted by simulations,

ISBN 978-3-95450-123-6

evidence of multipacting resonances in the cavity was detected at low power, and a wide multipacting-free region around the nominal operation point was confirmed. During the conditioning, the RF was first run in pulsed mode with 10% duty cycle. This approach allowed to "jump" the low power multipacting resonances by going directly to about half of the nominal power. From that point on, the peak power was first quickly increased up to the nominal value, and then the duty cycle was gradually increased up to CW operation.

Unexpected multipacting modes, in the $\sim$ 80 cm long (half an RF wavelenght) RF feeder coaxial lines between the RF windows and the cavity couplers (indicated as "RF Couplers" in Figure 1), were successfully cured by wrapping solenoids providing $\sim$ 50 Gauss field to this region of the coaxial lines.

Dark Current Characterization

Initial dark current characterization was performed in two phases. First, a coaxial Faraday cup was installed right at the gun beam exit pipe at $\sim$ 15 cm from the cathode. Figure 7 shows an example of a dark-current measurement with the Faraday cup, and a Fowler-Nordheim fit of the data. The fitting function is averaged over the RF period to account for the time variable fields in the cavity [29]. With the gun running in CW at the nominal power, $\sim$ 8 μA average current was measured. At a later time, the Faraday cup was moved to its present position at the end of the Phase 0 beamline $\sim$ 2 m downstream of the cathode. In this new configuration, the dark current transported to the Faraday cup is partially collimated out by the vacuum chamber and the measured value drops down to less than a μA when the gun is operated in CW mode at the nominal power. Initial studies show that the measured values of dark current should be compatible with the operation of a high repetition rate X-ray FEL [18].

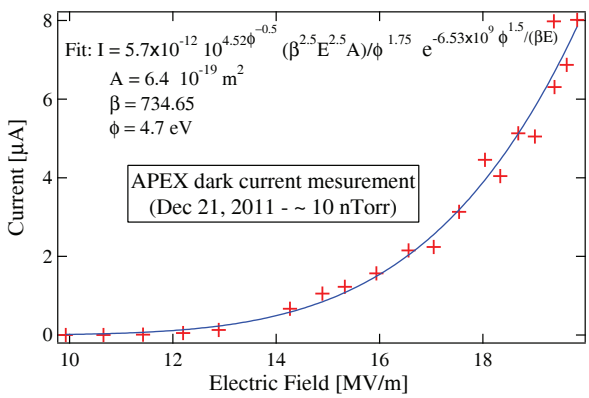

Figure 7: Example of dark current measurement and Fowler-Nordheim fit.

By imaging the dark current on a YAG screen using a solenoid in the transport line, it was observed that the field emission is mainly generated by few point-like sources on the cathode plane. In the present configuration, optimized for RF tests, a "dummy" molybdenum plug is installed instead of a real cathode. The better polishing level of a real cathode plug, and if required, a better cleaning technique to remove particulates [30], and/or a conditioning of the gun at higher RF fields [31] could potentially reduce dark current intensity.

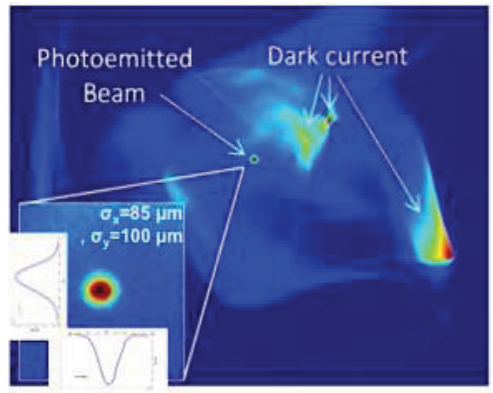

Figure 8: Example of image of the photoemitted beam on the YAG screen in the Phase 0 beamline.

Electron Beam Measurements

The dummy molybdenum cathode plug, used during this first commissioning, ensured the proper RF contact but presented a poor (estimated) QE of $\sim 10^{-6}$ at 266 nm. With the available laser power and that QE, the expected photoemitted charge per bunch is $\sim$ 6 fC that, with the MHz repetition rate, will generate an expected average current of 6 nA. Despite these challenging expectations, in March, 2012 the laser was synchronized with the gun RF by the LLRF system, and the photo-emitted beam was visualized on the YAG screen of the Phase 0 beamline.

Figure 8 shows an example of such a measurement.

In an another measurement, by using a lock-in amplifier with the cathode drive laser (MHz) trigger as reference, an average current of $\sim$ 10 nA was measured at the Faraday cup at the end of the beamline in fair agreement with the expected value (Fig. 9). In this measurement the RF phase in the gun was varied and the value measured with the laser shutter closed and open. The lock-in amplifier was triggered in phase with the laser and, since it is a phase sensitive instrument, varying the rf phase respect to the laser would vary also the value measured even in absence of photobeam. Indeed the dark current value changes with the injection phase.

Another fundamental milestone for the project was achieved few days after the first photoemitted beam with the demonstration of the design electron beam energy. A schematic of the beamline components used during the measurement is shown in the bottom part of Figure 10. The

ISBN 978-3-95450-123-6

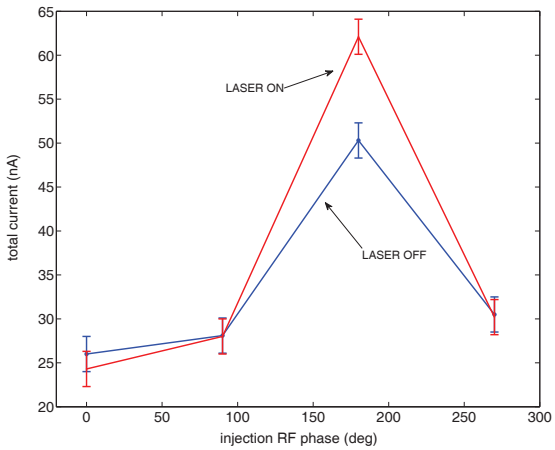

Figure 9: Measurement of photobeam current with a lockin amplifier triggered by the laser.

beam was focused on the beamline YAG screen by properly tuning the field in the first solenoid ("Sol.1" in the Figure). A horizontal corrector 0.443 m upstream of the screen ("Hor. Corr. 2" in the Figure) was subsequently energized at several different values and the beam centroid translation on the screen was recorded. An example of such a measurement is shown in the top part of Figure 10. The slope of the fit is proportional to the particle momentum and the measured energy value was 745 keV with a standard deviation of 41 keV, when the nominal RF power of 100 kW was applied to the cavity. Such a value is in excellent agreement with the expected 750 keV, confirming again the capability of the gun to generate the required fields.

Gun "RF Baking" and Vacuum Performance

The achievement of the required vacuum performance is of fundamental importance for the VHF gun to operate with semiconductor cathodes sensitive to contamination and ion back-bombardment with acceptable lifetime.

The VHF gun has been designed to withstand high temperature vacuum baking (lower than 400 °C). In the conventional scheme, the vacuum chamber to be baked is wrapped with heating tapes and maintained at temperatures higher than about 150 °C for many hours to allow the desorption of gas molecules from the chamber walls. One limitation of such a scheme is that components included inside the external chamber under baking are heated only by conduction through their connection to the chamber itself. This situation can result in a difficulty in control of the actual temperature of these internal parts. In order to overcome this situation, we used for the VHF gun a technique that we named as "RF baking". In such a procedure, the water cooling of the gun is turned completely off and a few kW of average RF power are applied to the cavity. Without water, the temperature of the cavity walls rises and can be easily maintained at the desired level by adjusting the RF power level. In this way, the RF conducting surfaces that most

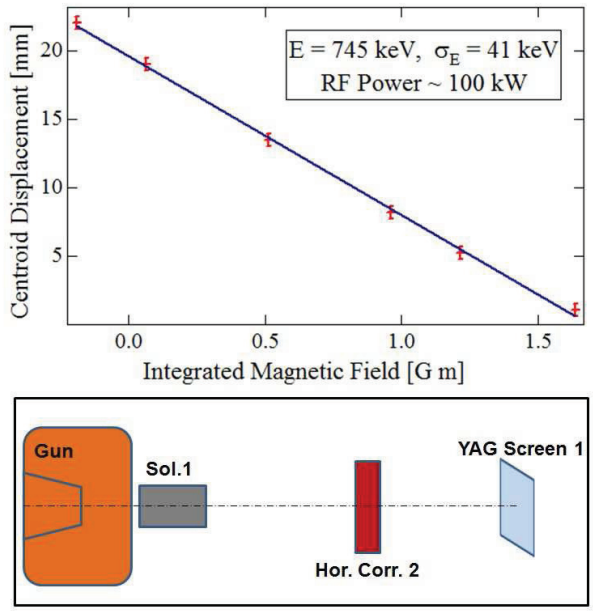

Figure 10: Top: example of photo-emitted electron beam energy measurement. The design value for the nominal RF power of 100 kW is 750 keV in excellent agreement with the measured value. Bottom: schematics of the layout used for the measurement.

need to be heated are brought to the desired temperature and a more effective vacuum baking is achieved.

Figure 11 shows the temperatures in different parts of the VHF gun during the "RF Baking" demonstration experiment we performed. All the gun parts were stably maintained between 130 and 180 °C for about 2.5 days with a turbo-molecular pump on. At the end of the period, the RF was switched off, the cavity ion pump was switched on, and one out of the twenty NEG modules was activated.

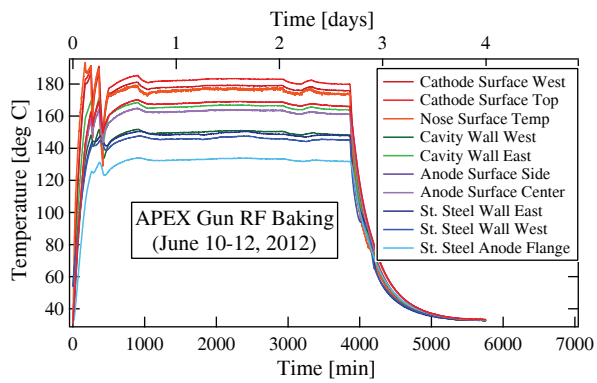

Figure 11: Temperatures in different parts of the VHF gun during a ~ 2.5 day "RF Baking" (see text for details).

Figure 12 shows a plot with the vacuum pressure inside the cavity (blue trace) and in proximity of the two RF windows in the couplers (red and green traces) after cooling down from the baking shown in Figure 11. The

ISBN 978-3-95450-123-6

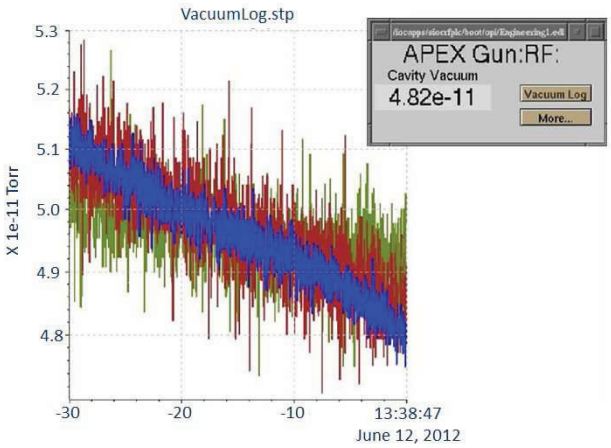

Figure 12: Plot of the vacuum pressure inside the gun cavity after the RF baking shown in Figure 11.

pressure value inside the cavity was below 5×10^{-11} Torr ($\sim 6.5 \times 10^{-8}$ Pa) and a clear trend towards even lower pressures is clearly visible. The pressure inside the couplers, which were not significantly heated during RF baking, was about one order of magnitude higher than in the cavity.

The described RF baking procedure will be repeated after the installation of the vacuum load-lock and a larger number of NEG pumps will be activated to achieve the ultimate vacuum performance of the gun.

CONCLUSIONS AND FUTURE PLANS

The commissioning of the APEX photogun has been completed. The fundamental milestones for this phase of the APEX project have been successfully demonstrated showing the capability of the gun to generate MHz repetition rate electron beams at the design energy. An excellent base vacuum pressure in the gun has been also achieved paving the way for the tests of semiconductor photocathodes as scheduled in the next phases of the project.

Additional future activities include the addition of a beam diagnostic suite to perform a 6D phase space characterization of the electron beam firstly at the gun energy, and subsequently at several tens of MeV for the final brightness performance demonstration of the gun when integrated in a full injector scheme.

It is worth remarking that in principle, repetition rates as high as the RF frequency can be achieved by the VHF gun, and that the actual repetition rate is limited by the available laser power used to drive the photocathode. Modified versions of the gun resonating at higher frequencies (< 700 MHz) may be used for ERL (energy recovery linac) applications.

ACKNOWLEDGEMENTS

The authors want to thank John Byrd, Peter Denes, Paul Emma, David Robin and the AFRD, ALS and Engineering Divisions for the continuous support during the various phases of the project, and Marco Venturini, Ji Qiang and Weishi Wan for useful discussions. The authors want also to express their appreciation to Ali Nassiri for his helpful participation to some of the commissioning shifts.

REFERENCES

[1] J. Corlett,*et al.*, Synchrotron Radiation News **22**, No. 5, 25 (2009).

[2] J. Bisognano, *et al.*, *The Wisconsin Free Electron Laser Initiative*, in proceedings of PAC09, Vancouver, BC, p. 109 (2009).

[3] R. Bartolini, *et al.*, *Optimisation of a Single-Pass Superconducting Linac as a FEL Driver for the NLS Project*, in proceedings of FEL2009, Liverpool, UK, p. 480 (2009).

[4] K.-J. Kim, S. Reiche, Y. Shvydko, Phys. Rev. Letters **100**, 244802 (2008).

[5] See for example: E. Arenholz, *et al.*, *Toward Control of Matter: Basic Energy Science Needs for a New Class of X-Ray Light Sources*, Proc. of the Science for a New Class of Soft X-Ray Light Sources Workshop, Berkeley, CA, October 8-10, 2007, LBNL Report LBNL-1034E (September 24, 2008).

[6] See for example: C. Limborg-Deprey, D. Dowell, J. Schmerge, Z. Li, and L. Xiao, *RF Design of the LCLS Gun*, LCLS TN-05-3, February 2005, or, S. Rimjaem, *et al.*, in Proceedings of the 2009 FEL Conference, Liverpool, UK, August 23-28, 2009, p. 251.

[7] J. W. Staples, S. P. Virostek, and S. M. Lidia, in Proceedings of the 2004 European Particle Accelerator Conference, Lucerne, Switzerland, July 5-9, 2004, p. 473.

[8] See for example: F. Sannibale, *Overview of Recent Progress on High Repetition Rate, High Brightness Electron Guns*, to appear in proceedings of IPAC12, New Orleans, LA USA May 2012, and references therein.

[9] F. Sannibale, D. Filippetto, and C. F. Papadopoulos, Journal of Modern Optics **58**, 1419 (2011).

[10] F. Sannibale, *et al.*, *Status of the LBNL normal-conducting CW VHF electron photo-gun*, in Proceedings of the 2010 FEL Conference, Malmö, Sweden, August 23-27, 2010, p. 475.

[11] J. W. Staples, F. Sannibale, S. Virostek, *VHF-band photoinjector*, CBP Tech Note 366, 2006.

[12] K. Baptiste, *et al.*, Nucl. Instrum. Methods Phys. Res., Sect. A **599**, 9 (2009).

[13] C. Reece, *et al.*, in Proceedings of the 1995 Particle Accelerator Conference and International Conference on High Energy Accelerators, Dallas TX, USA, p. 1512 (1995).

[14] B. Aune, *et al.*, Phys. Rev. ST Accel. Beams **3**, 092001 (2000).

[15] P. Michelato, C. Pagani,and D. Sertore, Private communications.

ISBN 978-3-95450-123-6

[16] C. F. Papadopoulos, *et al.*, *Multiobjective Optimization for the Advanced Photoinjector Experiment (APEX)*, in Proceedings of the 2010 FEL Conference, Malmö, Sweden, August 23-27, 2010, p. 479.

[17] See for example: L. Monaco, *et al.*, *Dark current investigation of FLASH and PITZ RF guns*, in Proceedings of EPAC06, Edinburgh, Scotland, p.2493 (2006), or D. H. Dowell, *et al.*, *Measurement and analysis of field emission electrons in the LCLS gun*, in Proceedings of the PAC07 Conference, Albuquerque, NM, USA, p. 1299 (2007).

[18] C. A. Steier, *et al.*, *Electron Beam Collimation for the Next Generation Light Source* to appear in proceedings of IPAC12, New Orleans, LA USA May 2012.

[19] D. Filippetto, *et al.*, *Low Energy Beam Diagnostic for APEX, the LBNL VHF Photo-injector*, in Proceedings of the 2011 PAC Conference, New York NY, US, p. 1903 (2011).

[20] I. V. Bazarov, *et al.*, Journal of Applied Physics **103**, 054901 (2008).

[21] S. Belomestnykh, *et al.*, Nuclear Instruments and Methods in Physics Research A **614**, 179 (2010).

[22] J. Power, *et al.*, *Upgrade of the Drive LINAC for the AWA Facility Dielectric Two-Beam Accelerator*, in Proceeding of IPAC10, Kyoto, Japan, p. 4310 (2010).

[23] R. A. Rimmer, *et al.*, *A Third-Harmonic RF Cavity for the Advanced Light Source*, in Proceeding of EPAC98, Stockholm, Sweden, p. 1808 (1998).

[24] J. Feng, *et al.*, *Drive Laser System for the Advanced Photo-Injector Project at the LBNL* in Proceedings of the 2011 PAC Conference, New York NY, US, p. 2537 (2011).

[25] T. Vecchione, *et al.*, Applied Physics Letters **99**, 034103, (2011).

[26] S.Zhou, et al, Applied optics **46**, 8488 (2007).

[27] C. Pogue, *et al.*, *Longitudinal Pulse Shaping of APEX Drive Laser*, these Proceedings.

[28] G. Huang, *et al.*, *LLRF Control Algorithm for APEX*, to appear in Proceedings of the 2012 IPAC Conference, New Orleans LA, US, (2012).

[29] See for example: J. W. Wang thesis, *RF properties of periodic accelerating structures for linear colliders*, SLAC-339 UC-28 (A), July 1989.

[30] See for example: D. Reschke, *et al.*, *Dry-ICE Cleaning: The Most Effective Cleaning Process for SRF Cavities*, in Proceedings of the 2007 SRF Conference, Beijing, China, p. 239 (2007).

[31] See for example: J. Norem, *et al.*, Phys. Rev. Special Topic, Acc. and Beams **6**, 072001 (2003).

ISBN 978-3-95450-123-6